Chemical Physics Letters 787 (2022) 139283

Contents lists available at ScienceDirect

Chemical Physics Letters

journal homepage: www.elsevier.com/locate/cplett

Implementing machine learning for the identification and classification of compound and mixtures in portable Raman instruments

Travon Cooman [a], Tatiana Trejos [a], Aldo H. Romero [b], Luis E. Arroyo [a,*]

[a] Department of Forensic and Investigative Science, West Virginia University, United States
[b] Physics and Astronomy Department, West Virginia University, United States

ARTICLE INFO

Keywords:
Machine learning
Neural networks
Portable Raman spectrometer
Seized drugs

ABSTRACT

Portable Raman instruments provide quick, nondestructive analysis of organic and inorganic compounds, making it widely applicable in various disciplines. However, the instrument's accuracy when analyzing pure, or multiple component mixtures is still an aspect that needs improvement. This study explored machine learning algorithms to classify single compounds, binary, ternary, and quaternary mixtures by the compound name, and the compound's class, using seized drugs and common diluents as a model. The accuracies were $\geq$ 93% for most pure, binary mixtures, and quaternary mixtures algorithms. Therefore, incorporating machine learning algorithms in portable instruments, can improve the detection of unknown substances with high accuracies.

1. Introduction

Portable instruments are becoming more prevalent due to their ability to provide quick results on-the-spot [1–3]. While data can be acquired in a short time, the specificity and accuracy of these instruments and the safety of the operators remain important. Portable analytical techniques for on-site applications include electrochemical systems [4], paper-based analytical devices [5,6], mass spectrometry methods [7], and spectroscopy methods [8]. In particular, scenarios where analysis requires packages to be opened at point-of-contact areas, the risk of exposure to unknown substances by personnel remains high. Raman spectroscopy provides unique advantages over other techniques due to its ability to be noninvasive [9] and even to analyze substances through packaging [10,11], thereby minimizing the risk of exposure to operators. For example, the Agilent Resolve Handheld Raman—a spatially offset Raman spectrometer (SORS) which allows subsurface analysis, is capable of analyzing explosives, drug precursors, toxic industrial chemicals, chemical warfare agents, and narcotics through packaging such as colored plastic and glass, paper, sacks, cardboard and fabric [11]. Conventional Raman systems are better suited for analysis through clear plastic bags and vials, and translucent packaging. Portable Raman systems have proved useful for the molecular identification of minerals [12], analysis of biomaterials [13], food quality monitoring [14,15], and analysis of drugs [3,16]. Raman spectroscopy is broadly applied in chemistry, biochemistry, biology, and medicine [17] due to its ability to provide a structural fingerprint by which molecules can be identified. Nonetheless, the instrument's accuracy is dependent on the incorporated algorithms that return an identification for an unknown compound.

Organic molecules, when stimulated by an excitation source such as a laser, results in a photon frequency shift due to the vibration produced by the interaction between the applied electromagnetic field and the electronic charge, which is unique to the molecule. Depending on the functional groups in the molecule, it may undergo symmetric, asymmetric stretching, or bending. These factors influence the Raman shifts and peak shapes and intensities observed in the resulting Raman spectrum. Unknown compounds can be compared to the vibrational signatures in a library. A common metric used for spectral comparisons is the hit quality index (HQI) where 1.0 represents a perfect correlation and 0.0 represents poor correlation [18]. A threshold for a 'match' or 'no match' result can be predetermined by the user based on the application. For example, in forensic science where mixtures are commonly encountered in seized drugs, a threshold of 85% for the HQI may be selected, but in the pharmaceutical industry where purer substances are encountered, the threshold might be 95% [19]. Spectra can be preprocessed to reduce the baseline by computing the first derivative to allow for higher discrimination [18]. One drawback to using the HQI is that incorrect identifications of similar compounds with small spectra differences may result [20]. Other metrics for spectral comparison include Pearson's correlation—where a value of 1 represents a perfect

* Corresponding author.
E-mail address: luis.arroyo@mail.wvu.edu (L.E. Arroyo).

https://doi.org/10.1016/j.cplett.2021.139283
Received 29 October 2021; Received in revised form 4 December 2021; Accepted 7 December 2021
Available online 10 December 2021

correlation and −1 represents a poor correlation, and cosine similarity—where 0 represents poor correlation and 1 represents perfect correlation [21]. However, these methods work well when there is a linear relationship between spectral features but can perform poorly with complex spectra of multiple mixtures.

One method used to recognize spectral features, otherwise difficult to visualize by the naked eye, is machine learning. Developed algorithms are trained to extract relevant features or patterns in complex spectra and predict the classes of new compounds, thereby improving detection, identification, and classification. Several supervised and unsupervised algorithms have been used in combination with spectroscopic data, including principal component analysis, k-nearest neighbors (kNN), random forests (RF), support vector machines (SVM) and deep learning methods [22–24].

Deep learning methods— an important branch of machine learning, are becoming more prevalent over traditional classification methods due to their ability to extract relevant information about labeled data in more complex datasets which contain non-linearly separable classes. Two algorithms used for Raman spectroscopy include artificial neural networks (NN) and convolutional neural networks (CNN) which are mathematically modeled after the nervous system [25]. CNNs are preferably used for image classification and object recognition over NNs—which can lead to overfitting, making CNNs ideal for spectral comparison [26] as spectra can be considered fingerprints of molecules or crystalline materials. A smart Raman spectrometer was developed to analyze pure compounds, binary and ternary mixtures with 99.9%, 96.7%, and 85.7% accuracy, respectively using a CNN [27].

Whereas many of these techniques have been used post acquisition of the spectra [24,28–32], few have incorporated these methods in portable Raman instruments [19,33]. Additionally, the combination of existing spectral comparison methods with classification techniques have not been explored. When machine learning algorithms are utilized, the main goal is to report a compound, but misclassification is common when new compounds are absent from the instrument's library, or the trained model has not seen the new compound.

In this study, we evaluate the accuracy of six machine learning algorithms— kNN, naïve bayes (NB), RF, SVM, NN, and CNN, on pure drug spectra, binary, ternary and quaternary mixtures and compare their accuracy to a recently validated portable Raman instrument which uses a HQI algorithm [34]. The findings presented here can be easily adapted to many other materials and applications.

2. Methods

2.1. Spectra acquisition

Spectra were acquired using a TacticID portable Raman spectrometer with a 300 mW, 785 nm laser, and 9 cm^{-1} resolution (B&W Tek, Newark, DE). As previously described [34], spectra were measured for 14 drugs and 15 diluents (**Supplementary Table 1**), using a laser power of 60 and 90%. The powder sampled were measured through glass vials and 2 mil plastic bags. A total of 444 pure spectra were collected.

The spectra were baseline corrected and truncated to include Raman shifts from 176 to 2000 cm^{-1}. A Savitsky-Golay filter was applied to smooth the spectra with a 5 point window length and third order polynomial.

2.2. Spectral comparison

The cosine similarity and Pearson's correlation were used to compare an authentic test set of pure compounds (referred to as authentic pure set). These compounds included acetaminophen, benzocaine, boric acid, caffeine, diphenhydramine, levamisole, lidocaine, maltose, mannitol, myo-inositol, phenacetin, and procaine. Spectra were acquired in triplicate through 2 mil plastic bags and the instrument was operated at 90% power. A second database was created comprising of the first derivative of the spectra from Section 2.1 and comparisons to the test spectra were reported.

2.3. Pure spectra algorithms

Data augmentation is common when spectra are limited for training machine learning algorithms (MLA) [30]. Therefore, 444,000 spectra were created by multiplying each spectrum by 1000 random numbers between 0 and 1. This introduced variation in the spectra and simulated instances where there might be suppression of signals, hence training the algorithms under the worst-case scenario. Each spectrum was normalized to its maximum intensity.

Six machine learning algorithms including k-nearest neighbors (kNN), naïve bayes (NB), support vector machine (SVM), random forest (RF), neural network (NN), and convolutional neural network (CNN) were explored. *Scikit-learn v 0.24.1* [35] in python was used for kNN, NB, SVM and RF classifiers. NN and CNN were based on *Keras v 2.4.0* with *Tensorflow v 2.4.1* backend [36]. Two models were created for each algorithm—one based on the compounds (n = 29) where the output is the compounds listed in **Supplementary** Table 1 and the second based on the compounds' class (n = 17), also listed in **Supplementary** Table 1**.** Training was performed on 80% of the data in each class and testing on 20% using the *stratify* argument in the *train_test_split* function in *Scikit-learn*. The optimized parameters for all machine learning algorithms can be found in the supplementary document.

The authentic pure set was used to evaluate the models. Two drugs—diphenhydramine (antihistamine), and mannitol (sugar) were not included in the training data and misclassification of these substances were expected with the models trained based on the compounds. However, we evaluated their classification based on the drug class.

2.4. Binary mixture algorithms

Simulated binary mixtures of the drugs and diluents from Section 2.2 were created using Eq. (1).

$$Mixture = (drug^{*}r) + (diluent^{*}(1 - r)) \quad (1)$$

Where r = [0.05, 0.10, 0.15, 0.20, 0.25, 0.30, 0.35, 0.40, 0.45, 0.50, 0.55, 0.60, 0.65, 0.70, 0.75, 0.80, 0.85, 0.90, 0.95], drug and diluent are the spectrum of each drug or diluent, respectively, and mixture is the resulting spectrum. Machine learning algorithms including SVM, kNN, CNN, NN, NB and RF were first evaluated on this simulated dataset (binary mix #1). A second dataset (binary mix #2) was created by applying a Fast Fourier transformation (FFT) to the spectra and multiplying each intensity by a random number between 0.8 and 1.2 as an additional data augmentation technique, adding unequal variation to the spectra. The two datasets were combined, and algorithms were selected to evaluate the data based upon the reported accuracy on binary mix #1 and the time taken to train the models. Therefore, NB was not selected due to poor accuracy and RF due to longer training times. The combined binary mixtures dataset contained 1,152,312 spectra with 224 unique binary compound mixtures and 88 binary compound class mixtures. A list of the mixtures can be found in **Supplementary Table 2.** Model parameters can also be found in the supplementary document.

To demonstrate the accuracy of the models, spectra from authentic in-house binary drug: diluent mixtures (n = 186) previously acquired using the TacticID instrument [34] were used to evaluate the algorithms and to compare with the instrument's reported results. The drug: diluent ratios were 1:4, 1:7, 1:10, and 1:20. As an example, for a 1:7 ratio, 10 mg of the drug and 70 mg of the diluent were mixed prior to analysis. Selected classifiers which included SVM, kNN, NN, and CNN were used to test the authentic in-house mixtures. The accuracy of the predictions was based on the three highest probabilities that a compound belonged to a class.

2.5. Ternary mixtures

Selected ternary mixtures were created from the spectra in Section 2.1. using Eq. (2).

$$TernaryMixture = (drug*0.05) + \left(diluent1*\frac{(1-0.05)}{2}\right) + \left(diluent2*\frac{(1-0.05)}{2}\right) \quad (2)$$

The resulting spectra were processed using the Fast Fourier Transformation (FFT) and multiplied by a random number between 0.8 and 1.2 as a data augmentation technique which introduced unequal variations in peak intensities. A total of 829,440 spectra were created and there were 60 ternary compound mixtures and 50 ternary compound class mixtures. A list of the mixtures can be found in **Supplementary**

Table 3 and 4. The evaluated algorithms included CNN, kNN, NN, and SVM. Additional information about the architecture of the models can be found in the supplementary document.

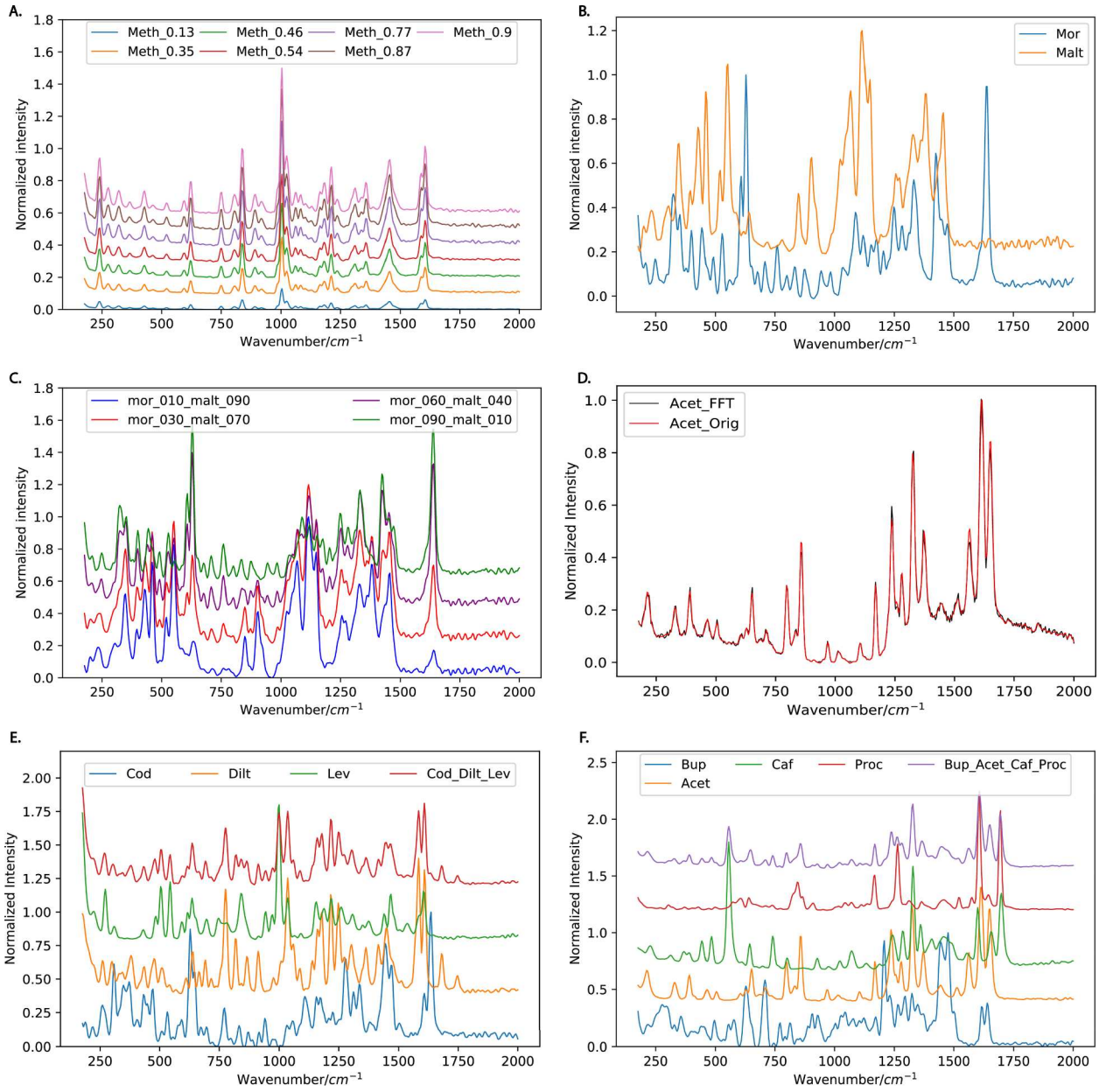

Fig. 1. (A)– Illustration of the resulting spectra when a methamphetamine (Meth) spectrum is multiplied by 0.13, 0.35, 0.46, 0.54, 0.77, 0.87, 0.90. (B)–Comparison of maltose (Malt) and morphine (Mor) spectrum. (C)– Illustrations of the resulting simulated spectra for morphine (multiplied by 0.1, 0.3, 0.6, 0.9) and maltose (multiplied by 0.9, 0.7, 0.4, 0.1). (D)– The spectrum of acetaminophen before (Acet_Orig) and after Fast Fourier transformation (Acet_FFT). (E)–Creation of a ternary mixture of codeine, diltiazem, and levamisole with the codeine signal suppressed to 5% of the original spectrum. (F)–Creation of a quaternary mixture containing buprenorphine, acetaminophen, caffeine, and procaine with 5% suppression of the buprenorphine signal.

2.6. Quaternary mixtures

Three subsets of quaternary mixtures were created from the spectra in **Section 2.1** using Eq. (3). The value 0.05 was selected to simulate the effect of high signal suppression of the drug in comparison to the diluents, as is usually the case in street drug mixtures, although this methodology can be easily generalized to other compounds. The spectra were also processed using the FFT prior to evaluation using machine learning algorithms created for classification by compound mixture and compound class mixture. SVM, kNN, CNN and NN were used to evaluate the data.

Subset 1 contained 4 quaternary mixtures of cocaine with acetaminophen, diltiazem, and hydroxyzine. See **Supplementary Table 5** for additional information about the mixtures. A total of 663,552 spectra were created in this set.

Subset 2 comprised of 1,327,104 spectra. Quaternary mixture combinations were created with the drug as buprenorphine and naltrexone and the diluents as acetaminophen, caffeine, procaine, and maltose. This resulted in 8 compound mixtures and a complete description can be found in **Supplementary Table 6.**

The quaternary mixtures in subset 4 contained codeine and morphine as drugs, and acetaminophen, caffeine, lidocaine, maltose as diluents. A total of 8 compound mixture classes (**Supplementary Table 7**) were created with 1,327,104 spectra. A summary of the methods is shown in Supplementary Figure 1 and additional details about the architectures of the models can be found in the supplementary document.

$$QuaternaryMixture = (drug^{*}0.05) + \left(diluent1^{*}\frac{(1-0.05)}{3}\right) + \left(diluent2^{*}\frac{(1-0.05)}{3}\right) + \left(diluent3^{*}\frac{(1-0.05)}{3}\right) \quad (3)$$

3. Results

3.1. Spectra Creation and comparison

A visual representation of the pure simulated spectra and binary, ternary, and quaternary mixtures recreation is shown in Fig. 1. Mixtures were created to represent complex combinations of drugs and diluents that represent common street drugs as well as worst case scenarios. Multiplication of the pure spectra by numbers between 0 and 1 resulted in a relative suppression or scaling of the signal intensities (Fig. 1A**).** Fig. 1B shows the individual spectrum of maltose and morphine and the differences in the number, shape, and intensity of the peaks characteristic of each compound. When the mixtures were simulated, the peak at 1640 cm^{-1} for morphine decreased relative to the diluent— maltose, when the ratio of maltose to morphine was higher (Fig. 1C). For example, when the morphine spectrum was multiplied by 0.90 and the maltose spectrum multiplied by 0.10, then combined, the resulting spectrum demonstrated more features similar to morphine. Fig. 1D shows the effect of applying the Fast Fourier transformation to the spectra. Some peak intensities are higher whereas others are lower than those in the original spectrum. Additionally, noise is added in random portions of the spectrum. Fig. 1E and 1F demonstrate the spectrum of a ternary and quaternary mixture, respectively. The deliberate suppression of the drug spectrum in relation to the diluents in both the ternary and quaternary mixture makes it difficult to identify the Raman bands unique to the drugs—codeine for the ternary mixture, and buprenorphine for the quaternary mixture.

The cosine similarity and Pearson's correlation coefficient for the authentic pure set is shown in Supplementary Figure 2. Although lower scores were observed when making comparisons of the first derivative spectra, all scores were greater than 0.90 with the cosine similarity, and greater than 0.86 with the Pearson's correlation. Comparisons on the pure test set using the cosine similarity resulted in methamphetamine having the highest similarity to diphenhydramine (0.820), and sorbitol having the highest similarity to mannitol (0.878). When comparisons were made using the first derivative algorithm combining the cosine similarity, the results were the same between mannitol and sorbitol, but the score was 0.640. Diphenhydramine was also most similar to fentanyl (0.717) using the first derivative comparison. The Pearson's correlation resulted in mannitol and sorbitol being most similar (0.817 and 0.640 for the original spectra and first derivative spectra algorithms respectively). Fentanyl and methamphetamine were also reported as the closest compounds to diphenhydramine. Although the first derivative provides lower correlation scores than the original spectral correlations, they are not markedly different.

3.2. Pure spectra

Exploratory analysis of the 444 pure spectra using PCA of the original spectra and the first derivative spectra is shown in Supplementary Figure 3**.** Plots of the first two principal components of the original spectra labeled by compound and class show overlap of the clusters making PCA a challenge for classification of this dataset. The explained variance in the first two components were 34% and 9%. Although some clusters are more separated when the first derivative of the spectra is computed (Supplementary Figure 3C, 3D), others still overlap. Linear discriminant analysis (LDA) results in higher separation of the classes, but overlap is still observed for few drugs and classes (Supplementary Figure 4). As a result, neither PCA nor LDA were used for further evaluation of the data in this study. Various machine learning algorithms were then evaluated in the pure spectra dataset, as explained below.

The performance of the method was evaluated as correct identification or accuracy. Correct identification was evaluated for the authentic datasets (pure and binary mixtures) where True positives and False negatives were considered. The models created from the simulated data were evaluated using accuracy. True positive, False positive, and their respective True negative and False negative were used in the calculation of accuracy (**Supplementary Equation** (1)).

The average accuracies of the kNN, RF and CNN algorithms for compound and compound class were 100% (Table 1). The SVM resulted in 99% accuracy for both models whereas the NN resulted in 98% for the compound model and 99% for the class model. The NB models resulted in the lowest accuracies for both models—68% for compound and 67% for compound class. Complete classification reports can be found in **Supplementary Tables 8 – 19**.

All models except the NB algorithm were used to evaluate the authentic pure set. Only the CNN resulted in 100% correct identification for both compound and class (Table 1)**.** This also included correctly classifying diphenhydramine and mannitol by compound class even though they were not included in the training data. However, they were misclassified by compound because the training data did not contain their labels. The RF model resulted in correct identifications of 97% for compounds and 94% for compound classes. The next best model—kNN, resulted in 93% correct identification for compounds and 86% for compound classes. The model with the lowest correct identification for reporting compounds and class was the SVM with 80% and 56%, respectively. Although at least 80% correct compound identification in

Table 1
Comparison of the algorithms' accuracy and evaluation of the models on an authentic pure test dataset. The pure test set accuracy is based on compound's presence in the top three hits.

	kNN		NB		RF		SVM		NN		CNN	
	Compound	Class	Compound	Class	Compound	Class	Compound	Class	Compound	Class	Compound	Class
Model Accuracy (%)	100	100	68	67	100	100	99	99	98	99	100	100
Pure Test Set Correct identification (%)	93	86	—	—	97	94	80	56	90	86	100	100

the top 3 hits was observed for all models, only the CNN resulted in the top hit corresponding to the ground truth compounds.

The accuracy and loss plots during training and testing of the CNN model are shown in Supplementary Figure 5. Although the model was created with 100 epochs, the implementation of early stopping to prevent overfitting meant that after 25 to 30 epochs, the training automatically stopped. The training accuracy remained between 99.7 and 99.9% after 5 epochs for the compound model (Supplementary Figure 5A). The testing accuracy fluctuated between 99.6 and 99.9% while the training loss continued to decrease from 0.030 to 0.005. A similar pattern was observed for the compound class model, but the testing accuracy fluctuated between 99.5 and 99.9% after 30 epochs.0.030 to 0.005. A similar pattern was observed for the compound class model, but the testing accuracy fluctuated between 99.5 and 99.9% after 30 epochs.

3.3. Binary mixtures

All models demonstrated at least 95% accuracy for compound mixtures or class mixtures except NB which had 47% accuracy with class mixtures (Table 2). The RF, NB and CNN all had 100% accuracy with the compound mixtures whereas only the RF, and CNN resulted in 100% accuracy for the class mixtures model.

Training for the CNN algorithm stopped after 17 and 16 epochs for the compound mixtures, and class mixtures model, respectively. Supplementary Figure 6 demonstrates an increase in training and testing accuracies while the loss decreased, indicating no overfitting.

3.4. Application to authentic In-house binary mixtures

The correct identification rates for the authentic in-house mixtures when using selected models was compared to results previously reported for the TacticID Raman [34]. The reported identification rates in Table 3 considers the presence of the ground truth in the top 3 hits. The top 3 hits were determined based on the classification probability as shown in Table 4. For example, a mixture containing morphine and maltose resulted in the correct mixture as hit #1 because of the highest probability they belonged to that class. However, the ground truth was reported as hit #2 in one instance (Table 4) with a probability of 0.003.

The authentic in-house mixtures were evaluated using the developed pure spectra algorithms to demonstrate the importance of model selection based on the application. The SVM and RF models resulted in the highest correct identifications for both drug and diluent in the top 3 hits—26% and 16%, respectively (Table 3). The SVM was the only algorithm that outperformed the HQI, with 51% correct identification for drug only compared to 30% with the HQI. Although, the Raman instrument does not report the class of unknown compounds, the pure spectra algorithms by compound class all provided correct identifications greater than 74% for diluents only and performed poorly for drug classification ($\leq$54%).

The correct identification improved when the binary mixtures models were used to assess the authentic in-house mixtures. All binary mixtures models demonstrated correct identifications at least double that which was observed with the Raman instrument (Table 5). Greater than 70% correct drug classification was observed for most algorithms compared to 30% with the HQI, and greater than 90% correct diluent classification for most algorithms as compared to 89% identification of the diluent with the HQI. Moreover, all the algorithms were able to correctly detect at least one compound or class in the mixture. The class mixtures correct identification rates cannot be compared with the Raman instrument because the instrument only reports the drug based on spectral similarity. However, the CNN and NN performed better than the other algorithms for drug class identification with 78% and 77%, respectively. The correct diluent class identification was $\geq$ 90% for all algorithms.

3.5. Ternary and quaternary mixtures

Molecular analysis of multiple component mixtures can be challenging using portable Raman spectroscopy as the signal of compounds in a lower percentage can be masked by compounds that are present in higher percentages. Therefore, investigating the performance of the algorithms on more complex mixtures is critical in understanding their applicability as screening tools.

In general, the tested algorithms successfully identified ternary mixtures. An example of the accuracy and validation loss plots during training and testing the ternary mixtures CNN algorithm is shown is Supplementary Figure 7. Training stopped after 16 – 20 epochs when the validation loss no longer decreased, and when the accuracy remained between 98.5% and 99.6%.

Evaluation of ternary mixtures using selected algorithms resulted in the kNN performing the worst with 83% accuracy for compound mixtures and 84% for compound class mixtures (Table 6). An accuracy greater than 95% was observed with all other models with the CNN's performance at 100%.

Interestingly, accuracy of identification of quaternary mixtures ranged from 93 to 100%, depending on the model and subset. The accuracy for all models on subset 1 was 100%, at least 99% on subset 2, and at least 93% on subset 3 (Table 7). The lowest accuracy for the compound mixtures model was observed with the NN.

4. Discussion

The CNN algorithm performed better than the other algorithms in detecting the authentic pure test compounds and their class with 100% correct identification (Table 1). The RF algorithm also produced a comparable but lower correct identification of 97%. The use of a *linear* kernel with the SVM models suggested our data was linearly separable due to the high accuracies observed in this study. The inclusion of a model trained by compound class proved to be useful in understanding the potential identity of an unknown compound when the HQI search results in no matches. This is particularly useful when Raman is used as a quick screening tool for drug identification. The two examples used in this study—diphenhydramine and mannitol, were correctly classified by their compound class using the CNN model, even though they were misclassified when tested using the compound model. Discrimination of three novel psychoactive substances (NPS) families—12 fentanyl related compounds, 8 synthetic cathinones, and 10 synthetic cannabinoids, was achieved using PCA [37]. The authors' intended use of this application was for law enforcement and customs officers where a diversity of controlled substances or counterfeits is encountered. The challenge with the use of PCA is when compounds of other drug families are

Table 2
Reported accuracy for the algorithms used to evaluate the simulated binary mixtures dataset. The NB and RF algorithms were only evaluated on binary mix #1 (spectra multiplied by numbers between 0.05 and 0.95).

	kNN		NB		RF		SVM		NN		CNN	
	Compound Mixtures	Class Mixtures	Compound Mixtures	Class Mixtures	Compound Mixtures	Class Mixtures	Compound Mixtures	Class Mixtures	Compound Mixtures	Class Mixtures	Compound Mixtures	Class Mixtures
Accuracy (%)	98	99	100	47	100	100	99	99	95	97	100	100

encountered, accuracy can suffer. We demonstrate in Supplementary Figure 3 the difficulty in separating multiple clusters using PCA and we believe it is not the ideal method for classification although it can be used for feature selection with other algorithms. LDA provided better class separation than PCA and reasonable accuracy (**Supplementary Table 20**)—96%, 88%, 91%, and 78% for single compounds, single classes, binary compound mixtures, and binary compound class mixtures, respectively, but emphasis was given to machine learning classifiers due to their higher accuracies with more complex datasets. Organic molecules which are structurally different by a functional group are of interest especially in forensic science, where new drug analogues are constantly emerging as a way of evading local laws and regulations. Although our study is not focused on differentiating between functional groups, a study using CNN demonstrated 100% accuracy in discriminating between toluene, aniline, o-xylene which differ by the number and position of a methyl group [30].

In many laboratories especially in forensic science, the ability to identify a controlled substance from seized materials using portable Raman instruments can provide more effective decision-making onsite and more efficient processing of cases at points of entry, such as customs. However, it is a challenge because most drug cases involve impure substances where the controlled drug is of a lower percentage making detection by conventional Raman difficult. For this reason the use of portable Raman is considered a screening tool requiring further confirmation using an additional technique. During a presumptive stage, accuracies above 70% are acceptable to inform the user about a potential drug or compound of interest. The rapid and non-destructive nature of portable Raman makes it an ideal technique to make quick sampling and investigative decisions at the point of contact, with minimal sample manipulation and under safe conditions to the operators. Similarly, in counterfeit pharmaceutical products, the high percentage of excipients may mask the active pharmaceutical ingredients. Therefore, we decided to calculate correct identification of the in-house binary mixtures test set based on its presence in the top three hits, accounting for uncertainties in classification. The instrument's accuracy for detecting the drug—a controlled substance in the mixtures, using the HQI algorithm was 30%, and lower than all the evaluated machine learning algorithms **(**Table 5**).** The NN and CNN models resulted in the highest correct identification rate—73% and 69% for drug only, and 65% and 64% for both compounds, respectively.

The success of the CNN algorithm for pure compounds and mixtures has been supported by several studies [22–24,27,29,30,32,38]. In one study, a smart Raman instrument was developed and the reported accuracy for ternary mixtures was 85.7% but 100% was observed with our CNN algorithm although the tested compounds were different [27]. The architecture of the CNN model reported by the authors contained 9 layers possibly due to the complexity of the acquired spectra, and incorporated dropout to prevent overfitting. Our CNN model consisted of no more than 5 layers, and without dropout as there was no indication of overfitting. Additionally, the authors only reported compound mixtures, but we also report compound class mixtures. However, despite the algorithm used, sampling is also important. Some studies used solvent mixtures which allows for a more homogeneous sampling which results in spectra that better represent the contents. Fan *et al* evaluated binary mixtures of polyacrylamide and sodium acetate but at a 1:1 ratio with a 100% true positive rate [23]. Our test mixtures included ratios of 1:4, 1:7, 1:10 and 1:20 where the controlled drug was present in a smaller percentage, simulating what can be expected in street drugs. The correct identification rates for the drug in the authentic mixtures decreased as the drug: diluent ratios increased with all algorithms, demonstrating the difficulty in detecting low concentration compounds in mixtures. Although, several measurements are required when performing analysis using portable Raman instruments to account for inhomogeneous samples, the acquired data may still be unrepresentative of the compounds in the mixture. One method that addresses this issue is the orbital raster scanning technique which allows the Raman instrument's laser to sweep

Table 3
Correct identification rates of the in-house binary mixtures dataset using the pure spectra algorithms for classification. The results are based on the presence of the mixtures in the top 3 hits.

	HQI	kNN		RF		SVM		NN		CNN	
Correct Identification (ID, %)		Compound Mixtures	Class Mixtures	Compound Mixtures	Class Mixtures	Compound Mixtures	Class Mixtures	Compound Mixtures	Class Mixtures	Compound Mixtures	Class Mixtures
Drug	30	24	19	24	42	51	54	15	12	30	22
Diluent	89	80	81	89	96	74	77	75	77	75	78
Drug and Diluent	19	5	1	16	38	26	32	2	1	5	1
At least one compound/ class	99	99	99	97	100	99	98	88	89	100	100

Table 4
Example of generated table for CNN drug algorithm evaluation on in-house mixtures. (Mor- morphine, malt- maltose, 4MEC- methylethcathinone, 4MMC- 4-methylmethcathinone).

Ground Truth	Hit #1	Hit #2	Hit #2	Hit #1 Probability	Hit #2 Probability	Hit #3 Probability
Mor– Malt	Mor–Malt	4MMC–Malt	4MEC–Malt	0.996	0.004	0.000
Mor–Malt	Mor–Malt	4MMC–Malt	4MEC–Malt	0.986	0.014	0.000
Mor–Malt	4MMC–Malt	Mor–Malt	4MEC–Malt	0.997	0.003	0.000

Table 5
Correct identification rates for the in-house binary mixtures using the simulated binary mixtures algorithms in comparison to the Raman instrument built-in hit quality index (HQI). The NB models were not evaluated as the other algorithms resulted in higher identification rates for both compound and compound class. The RF algorithm was not evaluated on the in-house mixtures. The correct identification was based on the true compound/ class being in the top 3 hits.

	HQI	kNN		SVM		NN		CNN	
		Compound Mixtures	Class Mixtures	Compound Mixtures	Class Mixtures	Compound Mixtures	Class Mixtures	Compound Mixtures	Class Mixtures
Drug (%)	30	59	60	61	73	73	77	69	78
Diluent (%)	89	90	90	94	95	92	95	95	93
Both (%)	19	49	50	55	68	65	72	64	72
At least one compound/Class (%)	99	100	100	100	100	100	100	100	100

Table 6
Accuracy of ternary mixtures models.

	kNN		SVM		NN		CNN	
	Compound Mixtures	Class Mixtures	Compound Mixtures	Class Mixtures	Compound Mixtures	Class Mixtures	Compound Mixtures	Class Mixtures
Accuracy (%)	83	84	99	99	95	99	100	100

Table 7
Accuracy of quaternary mixtures models.

	kNN		SVM		NN		CNN	
	Compound Mixtures	Class Mixtures	Compound Mixtures	Class Mixtures	Compound Mixtures	Class Mixtures	Compound Mixtures	Class Mixtures
Subset 1 Accuracy (%)	100	100	100	100	100	100	100	100
Subset 2 Accuracy (%)	100	100	100	100	99	100	100	100
Subset 3 Accuracy (%)	97	100	99	100	93	100	99	100

over large areas of the sample to yield an average spectrum [39,40]. However, evaluating the accuracy of this technique with machine learning would have to be studied and compared to conventional Raman instruments. The simulated complex mixtures data demonstrated that if measurements capture all components in a sample, the algorithm will detect them with high accuracy. An alternative to conventional Raman—surface enhanced Raman spectroscopy (SERS) requires collection of a small sample dissolved in a solvent prior to analysis. This technique can provide more representative information about the components of a mixture even when the target substance is in low quantities, but can be

risky when performed outside a controlled environment if the operator is exposed to unknown compounds [41–43].

A comparison of the effect of training with the mixtures models (Table 5) or pure models (Table 3) to predict the compounds in the test mixtures demonstrated the importance of having the appropriate model in the library. For example, if ternary mixtures are being tested, the models should be trained on ternary mixtures. If the pure model which returns a single compound is used on mixtures, a result for the compound most representative of the spectrum will result, as demonstrated by the accuracy of the diluent in Table 3. Additionally, the algorithms detected differences in spectra of ternary and quaternary mixtures, that would otherwise be challenging to observe by inspection, with high accuracies (~83–100%, Table 6 and 7). Depending on the application, if the number of component mixtures is known, algorithms can be designed to meet this expectation. For example, if the number of mixtures in street drugs does not typically exceed 5 compounds, then training algorithms to detect more than 4 components would not be necessary.

We propose the use of models created to report single compounds, single compound classes, binary, ternary, and quaternary mixtures using the CNN algorithm due to the high correct identification rates and accuracy reported in this study. Instead of implementing these classification techniques post processing, they can be incorporated into portable instruments and depending on the application, provide both spectral correlation information using the HQI, cosine similarity or Pearson's correlation, and classification as demonstrated by the proposed workflow in Fig. 2. One advantage of this classification and reporting workflow, is the gain of feedback to the end-user. When the identity of a

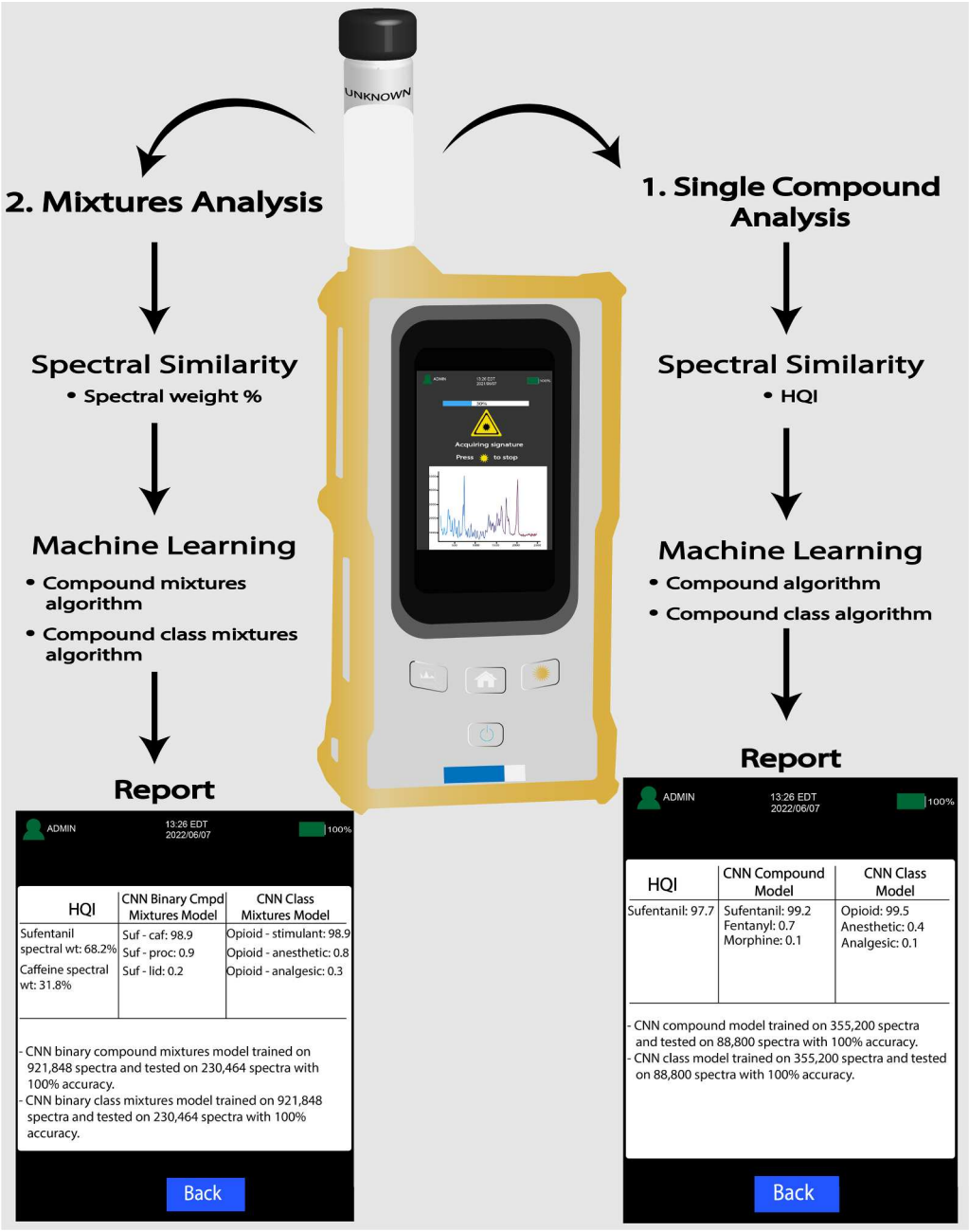

Fig. 2. An example of a workflow that can be implemented in portable Raman instruments. If the intended application requires a numerical value for spectral correlation, a similarity metric can provide a HQI for pure compounds and spectral weight for mixtures. Machine learning algorithms can also be incorporated for identification of the compounds and their classes. In the final report, a summary of the potential hits and their respective class probabilities is reported.

compound is unknown and misclassified by the conventional HQI, having a built-in CNN algorithm can provide additional information about drug classes and potential mixtures. For example, when pure PB-22 was analyzed using the portable Raman instrument, it was reported as BB22 using the HQI due to the similarity between their spectra. Nonetheless, using the machine learning algorithm for compound class classified it as a synthetic cannabinoid even though it was absent from the library.

It should be noted that depending on the application, the proposed approach still has some limitations. For example, in the pharmaceutical industry where purer compounds are encountered and Raman is the primary technique used, instead of using the top three hits (Table 4), the top hit might be more important. On the other hand, in forensic science, where portable Raman is used as a screening method, it might be acceptable to consider the top three hits as potential compounds since confirmation using a secondary technique would be required before reporting components of seized materials. One of the drawbacks of using machine learning algorithms on large datasets is that it requires high computing capabilities as observed with Random Forests in this study. However, given portable instruments such as the TacticID have Wi-Fi capabilities, access to a server can be used to train the algorithms on new data and be used to perform searches. In future studies, other data augmentation parameters such as Raman shift offset can be used in training the models to increase their robustness. Additionally, creation of authentic ternary and quaternary mixtures can be created to demonstrate the capability of the algorithms as more complex drug: diluent mixtures have previously reported in casework [44].

Machine learning which detects minor differences in spectra of complex mixtures outperformed the HQI algorithm incorporated in a portable Raman system. Implementation of machine learning algorithms capable of detecting single compounds, mixtures, and their classes can provide useful screening information about unknown compounds or molecules. Although, our proposed approach provides a probability for each hit, when needed, a spectral correlation technique can be used. Furthermore, having these methods built into the instrument eliminates the need to first export the data for post processing, and does not require separate libraries to be installed on the instrument as models can be trained offline then transferred to the device. Reporting the accuracy of the models as shown in Fig. 2, size of the training, and testing data results in more transparent reporting of results. The concept proposed in this study will therefore benefit applications where portable Raman instruments are used for compound screening including forensic science, medicine, and pharmaceutical industries.

5. Conclusion

Six machine learning algorithms—kNN, NB, RF, SVM, NN, and CNN were investigated and compared to a portable Raman instrument's accuracy in detecting pure powders, binary, ternary, and quaternary mixtures in this study. The CNN performed better than all algorithms with 100% correct identification for pure substances by compound and class. Both the NN and CNN resulted in superior correct identification on the authentic binary mixtures data— 65% and 64%, respectively in detecting both compounds in comparison to 19% observed in the portable Raman instrument. Improved accuracy in the binary simulated mixtures was observed, ranging from 83 to 100%, depending on the model and algorithm used, with superior performance observed for CNN. The CNN also provided the highest accuracy on the ternary and quaternary mixtures—100%, demonstrating its ability to provide compound and class information on samples that simulate common seized drugs formulations.

We propose the use of the HQI for spectral correlation and CNN models in portable Raman instruments to provide preliminary information about the identity of a compound and its class. Incorporating machine learning algorithms into portable Raman systems can enhance the response and feedback provided to law enforcement and scientists at the laboratory and onsite, facilitating more efficient and safer decision-making during sampling and investigative stages. The methods proposed here are broadly applicable to other materials and disciplines that use Raman spectroscopy as a rapid method for point-of-contact analysis.

Funding

This project was funded by National Institute of Justice Award #2019-DU-BX-0030. The opinions, findings, and conclusions are those of the authors and do not necessarily reflect those of the Department of Justice.

CRediT authorship contribution statement

Travon Cooman: Conceptualization, Methodology, Formal analysis, Investigation, Validation, Software, Writing – original draft, Writing – review & editing. **Tatiana Trejos:** Methodology, Writing – review & editing, Visualization. **Aldo H. Romero:** Conceptualization, Visualization, Resources, Supervision, Writing – review & editing. **Luis E. Arroyo:** Conceptualization, Resources, Visualization, Supervision, Project administration, Writing – review & editing.

Declaration of Competing Interest

The authors declare that they have no known competing financial interests or personal relationships that could have appeared to influence the work reported in this paper.

Acknowledgements

The authors thank Brianna Sauvé for assisting with acquiring Raman spectra. The authors are also grateful to the West Virginia University for the use of the Super Computing System (Thorny Flat), which is funded in part by the National Science Foundation (NSF) Major Research Instrumentation Program (MRI) Award #1726534.

Appendix A. Supplementary material

Supplementary data to this article can be found online at https://doi.org/10.1016/j.cplett.2021.139283.

References

[1] J.-P. Bourgeois, O. Vorlet, Low-cost portable Raman instrument, a tool toward counterfeit medication identification, Chim. Int. J. Chem. 72 (2018) 905–906.
[2] E.L. Izake, Forensic and homeland security applications of modern portable Raman spectroscopy, Forensic Sci. Int. 202 (2010) 1–8, https://doi.org/10.1016/j.forsciint.2010.03.020.
[3] W.R. de Araujo, T.M.G. Cardoso, R.G. da Rocha, M.H.P. Santana, R.A.A. Muñoz, E. M. Richter, T.R.L.C. Paixão, W.K.T. Coltro, Portable analytical platforms for forensic chemistry: A review, Anal. Chim. Acta. 1034 (2018) 1–21, https://doi.org/10.1016/j.aca.2018.06.014.
[4] J. Wang, Portable electrochemical systems, TrAC, Trends Anal. Chem. 21 (2002) 226–232, https://doi.org/10.1016/S0165-9936(02)00402-8.
[5] M.O. Salles, G.N. Meloni, W.R. de Araujo, T.R.L.C. Paixão, Explosive colorimetric discrimination using a smartphone, paper device and chemometrical approach, Anal. Methods. 6 (2014) 2047–2052, https://doi.org/10.1039/C3AY41727A.
[6] A.W. Martinez, S.T. Phillips, M.J. Butte, G.M. Whitesides, Patterned Paper as a Platform for Inexpensive, Low-Volume, Portable Bioassays, Angew. Chemie Int. Ed. 46 (2007) 1318–1320, https://doi.org/10.1002/anie.200603817.
[7] H. Brown, B. Oktem, A. Windom, V. Doroshenko, K. Evans-Nguyen, Direct Analysis in Real Time (DART) and a portable mass spectrometer for rapid identification of common and designer drugs on-site, Forensic Chem. 1 (2016) 66–73, https://doi.org/10.1016/j.forc.2016.07.002.
[8] E.M.A. Ali, H.G.M. Edwards, The detection of flunitrazepam in beverages using portable Raman spectroscopy, Drug Test. Anal. 9 (2017) 256–259, https://doi.org/10.1002/dta.1969.
[9] S. Pleus, S. Schauer, N. Jendrike, E. Zschornack, M. Link, K.D. Hepp, C. Haug, G. Freckmann, Proof of concept for a new Raman-based prototype for noninvasive glucose monitoring, J. Diabetes Sci. Technol. 15 (2021) 11–18.
[10] B. Cletus, W. Olds, E.L. Izake, S. Sundarajoo, P.M. Fredericks, E. Jaatinen, Combined time- and space-resolved Raman spectrometer for the non-invasive

depth profiling of chemical hazards, Anal. Bioanal. Chem. 403 (2012) 255–263, https://doi.org/10.1007/s00216-012-5792-2.
[11] Agilent Technologies, Agilent Resolve Raman, (n.d.). https://www.agilent.com/cs/library/brochures/5991-8867EN_Resolve_brochure_CPOD-web.pdf.
[12] J. Jehlička, H.G.M. Edwards, A. Culka, Using portable Raman spectrometers for the identification of organic compounds at low temperatures and high altitudes: Exobiological applications, Philos. Trans. R. Soc. A Math. Phys. Eng. Sci. 368 (2010) 3109–3125, https://doi.org/10.1098/rsta.2010.0075.
[13] M.D. Hargreaves, N.A. Macleod, V.L. Brewster, T. Munshi, H.G.M. Edwards, P. Matousek, Application of portable Raman spectroscopy and benchtop spatially offset Raman spectroscopy to interrogate concealed biomaterials, J. Raman Spectrosc. 40 (2009) 1875–1880, https://doi.org/10.1002/jrs.2335.
[14] G.Y. Tiryaki, H. Ayvaz, Quantification of soybean oil adulteration in extra virgin olive oil using portable raman spectroscopy, J. Food Meas. Charact. 11 (2017) 523–529.
[15] M.K. Nieuwoudt, S.E. Holroyd, C.M. McGoverin, M.C. Simpson, D.E. Williams, Rapid, sensitive, and reproducible screening of liquid milk for adulterants using a portable Raman spectrometer and a simple, optimized sample well, J. Dairy Sci. 99 (2016) 7821–7831, https://doi.org/10.3168/jds.2016-11100.
[16] C. Tondepu, R. Toth, C.V. Navin, L.S. Lawson, J.D. Rodriguez, Screening of unapproved drugs using portable Raman spectroscopy, Anal. Chim. Acta. 973 (2017) 75–81, https://doi.org/10.1016/j.aca.2017.04.016.
[17] M.D. Keller, E. Vargis, A. Mahadevan-Jansen, N. de M. Granja, R.H. Wilson, M.-A. Mycek, M.C. Kelley, Development of a spatially offset Raman spectroscopy probe for breast tumor surgical margin evaluation, J. Biomed. Opt. 16 (2011) 1–9, https://doi.org/10.1117/1.3600708.
[18] J.D. Rodriguez, B.J. Westenberger, L.F. Buhse, J.F. Kauffman, Standardization of Raman spectra for transfer of spectral libraries across different instruments, Analyst 136 (2011) 4232, https://doi.org/10.1039/c1an15636e.
[19] C.M. Gryniewicz-Ruzicka, J.D. Rodriguez, S. Arzhantsev, L.F. Buhse, J. F. Kauffman, Libraries, classifiers, and quantifiers: A comparison of chemometric methods for the analysis of Raman spectra of contaminated pharmaceutical materials, J. Pharm. Biomed. Anal. 61 (2012) 191–198, https://doi.org/10.1016/j.jpba.2011.12.002.
[20] K.A. Bakeev, R.V. Chimenti, Pros and cons of using correlation versus multivariate algorithms for material identification via handheld spectroscopy, Eur. Pharm. Rev. 1 (2013).
[21] A.Z. Samuel, R. Mukojima, S. Horii, M. Ando, S. Egashira, T. Nakashima, M. Iwatsuki, H. Takeyama, On selecting a suitable spectral matching method for automated analytical applications of Raman spectroscopy, ACS Omega 6 (2021) 2060–2065, https://doi.org/10.1021/acsomega.0c05041.
[22] S. Weng, H. Yuan, X. Zhang, P. Li, L. Zheng, J. Zhao, L. Huang, Deep learning networks for the recognition and quantitation of surface-enhanced Raman spectroscopy, Analyst 145 (2020) 4827–4835, https://doi.org/10.1039/D0AN00492H.
[23] X. Fan, W. Ming, H. Zeng, Z. Zhang, H. Lu, Deep learning-based component identification for the Raman spectra of mixtures, Analyst 144 (2019) 1789–1798, https://doi.org/10.1039/C8AN02212G.
[24] J. Acquarelli, T. van Laarhoven, J. Gerretzen, T.N. Tran, L.M.C. Buydens, E. Marchiori, Convolutional neural networks for vibrational spectroscopic data analysis, Anal. Chim. Acta. 954 (2017) 22–31, https://doi.org/10.1016/j.aca.2016.12.010.
[25] A. Abraham, Artificial neural networks, Handb. Meas. Syst. Des. (2005).
[26] I. Gogul, V.S. Kumar, Flower species recognition system using convolution neural networks and transfer learning, Fourth Int. Conf. Signal Process. Commun. Netw., IEEE 2017 (2017) 1–6.
[27] L.L. Chandler, B. Huang, T. Mu, A smart handheld Raman spectrometer with cloud and AI deep learning algorithm for mixture analysis, in: R.A. Crocombe, L.T. Profeta, A.K. Azad (Eds.), Next-Generation Spectrosc. Technol. XII, SPIE, 2019: p. 7. https://doi.org/10.1117/12.2519139.
[28] L.A. Reisner, A. Cao, A.K. Pandya, An integrated software system for processing, analyzing, and classifying Raman spectra, Chemom. Intell. Lab. Syst. 105 (2011) 83–90, https://doi.org/10.1016/j.chemolab.2010.09.011.
[29] M.H. Mozaffari, L.-L. Tay, Anomaly detection using 1D convolutional neural networks for surface enhanced raman scattering, in: SPIE Futur. Sens. Technol., International Society for Optics and Photonics, 2020: p. 115250S.
[30] M.H. Mozaffari, L.-L. Tay, Raman spectral analysis of mixtures with one-dimensional convolutional neural network, ArXiv Prepr. ArXiv2106.05316. (2021).
[31] S. Mazurek, R. Szostak, Quantification of atorvastatin calcium in tablets by FT-Raman spectroscopy, J. Pharm. Biomed. Anal. 49 (2009) 168–172, https://doi.org/10.1016/j.jpba.2008.10.015.
[32] X. Fu, L. Zhong, Y. Cao, H. Chen, F. Lu, Quantitative analysis of excipient dominated drug formulations by Raman spectroscopy combined with deep learning, Anal. Methods. 13 (2021) 64–68, https://doi.org/10.1039/D0AY01874K.
[33] S.R. Karunathilaka, B.J. Yakes, K. He, L. Brückner, M.M. Mossoba, First use of handheld Raman spectroscopic devices and on-board chemometric analysis for the detection of milk powder adulteration, Food Control 92 (2018) 137–146, https://doi.org/10.1016/j.foodcont.2018.04.046.
[34] T. Cooman, C.E. Ott, K.A. Dalzell, A. Burns, E. Sisco, L.E. Arroyo, Screening of seized drugs utilizing portable Raman spectroscopy and direct analysis in real time-mass spectrometry (DART-MS), Forensic Chem. 25 (2021), 100352, https://doi.org/10.1016/j.forc.2021.100352.
[35] E. Pedregosa, F. Varoquaux, G. Gramfort, A. Michel, V. Thirion, B. Grisel, O. Blondel, M. Prettenhofer, P. Weiss, R. Dubourg, V. Vanderplas, J. Passos, A. Cournapeau, D. Brucher, M. Perrot, M. Duchesnay, Scikit-learn: Machine learning in python, J. Mach. Learn. Res. 12 (2011) 2825–2830.
[36] M. Abadi, P. Barham, J. Chen, Z. Chen, A. Davis, J. Dean, M. Devin, S. Ghemawat, G. Irving, M. Isard, Tensorflow: A system for large-scale machine learning, in: 12th {USENIX} Symp. Oper. Syst. Des. Implement. ({OSDI} 16), 2016: pp. 265–283.
[37] J. Omar, B. Slowikowski, C. Guillou, F. Reniero, M. Holland, A. Boix, Identification of new psychoactive substances (NPS) by Raman spectroscopy, J. Raman Spectrosc. 50 (2019) 41–51, https://doi.org/10.1002/jrs.5496.
[38] J. Wahl, M. Sjödahl, K. Ramser, Single-step preprocessing of Raman spectra using convolutional neural networks, Appl. Spectrosc. 74 (2020) 427–438, https://doi.org/10.1177/0003702819888949.
[39] M.A. Mansouri, P.-Y. Sacré, L. Coïc, C. De Bleye, E. Dumont, A. Bouklouze, P. Hubert, R.D. Marini, E. Ziemons, Quantitation of active pharmaceutical ingredient through the packaging using Raman handheld spectrophotometers: A comparison study, Talanta 207 (2020), 120306, https://doi.org/10.1016/j.talanta.2019.120306.
[40] L. Coic, P.-Y. Sacré, A. Dispas, E. Dumont, J. Horne, C. De Bleye, M. Fillet, P. Hubert, E. Ziemons, Evaluation of the analytical performances of two Raman handheld spectrophotometers for pharmaceutical solid dosage form quantitation, Talanta 214 (2020), 120888, https://doi.org/10.1016/j.talanta.2020.120888.
[41] A. Haddad, O. Green, J.R. Lombardi, Detection of fentanyl in binary mixtures with cocaine by use of surface-enhanced Raman spectroscopy, Spectrosc. Lett. 52 (2019) 462–472, https://doi.org/10.1080/00387010.2019.1671871.
[42] A. Haddad, M.A. Comanescu, O. Green, T.A. Kubic, J.R. Lombardi, Detection and quantitation of trace fentanyl in heroin by surface-enhanced Raman spectroscopy, Anal. Chem. 90 (2018) 12678–12685, https://doi.org/10.1021/acs.analchem.8b02909.
[43] J. Leonard, A. Haddad, O. Green, R.L. Birke, T. Kubic, A. Kocak, J.R. Lombardi, SERS, Raman, and DFT analyses of fentanyl and carfentanil: Toward detection of trace samples, J. Raman Spectrosc. 48 (2017) 1323–1329, https://doi.org/10.1002/jrs.5220.
[44] T.R. Fiorentin, A.J. Krotulski, D.M. Martin, T. Browne, J. Triplett, T. Conti, B. K. Logan, Detection of cutting agents in drug-positive seized exhibits within the United States, J. Forensic Sci. 64 (2019) 888–896, https://doi.org/10.1111/1556-4029.13968.